HHS Public Access

Author manuscript

Acta Neuropathol. Author manuscript; available in PMC 2017 February 01.

Published in final edited form as:

Acta Neuropathol. 2016 February ; 131(2): 299–307. doi:10.1007/s00401-015-1532-y.

Gliomatosis cerebri in children shares molecular characteristics with other pediatric gliomas

Alberto Broniscer[1,6], **Omar Chamdine**[1], **Scott Hwang**[2], **Tong Lin**[3], **Stanley Pounds**[3], **Arzu Onar-Thomas**[3], **Sheila Shurtleff**[4], **Sariah Allen**[4], **Amar Gajjar**[1,6], **Paul Northcott**[5], and **Brent A. Orr**[4]

Alberto Broniscer: alberto.broniscer@stjude.org

[1]Department of Oncology, St. Jude Children's Research Hospital, 262 Danny Thomas Place, Memphis, TN 38105, USA

[2]Department of Diagnostic Imaging, St. Jude Children's Research Hospital, 262 Danny Thomas Place, Memphis, TN 38105, USA

[3]Department of Biostatistics, St. Jude Children's Research Hospital, 262 Danny Thomas Place, Memphis, TN 38105, USA

[4]Department of Pathology, St. Jude Children's Research Hospital, 262 Danny Thomas Place, Memphis, TN 38105, USA

[5]Department of Developmental Neurobiology, St. Jude Children's Research Hospital, 262 Danny Thomas Place, Memphis, TN 38105, USA

[6]Department of Pediatrics, University of Tennessee Health Science Center, 50 North Dunlap, Memphis, TN 38103, USA

Abstract

Gliomatosis cerebri (GC), a rare and deadly CNS neoplasm characterized by involvement of at least three cerebral lobes, predominantly affects adults. While a few small series have reported its occurrence in children, little is known about the molecular characteristics of pediatric GC. We reviewed clinical, radiological, and histological features of pediatric patients with primary GC treated at our institution over 15 years. Targeted sequencing of mutational hotspots in *H3F3A*, *IDH1/2*, and *BRAF*, and genome-wide analysis of DNA methylation and copy number abnormalities was performed in available tumors. Thirty-two patients [23 (72 %) with type 1 and 9 (28 %) with type 2 GC] were identified. Median age at diagnosis was 10.2 years (range 1.5–19.1). A median of 4 cerebral lobes (range 3–8) was affected at diagnosis. In addition, symmetrical bithalamic involvement was observed in 9 (28 %) patients. Twenty-two patients (69 %) had an anaplastic astrocytoma. Despite aggressive therapy, only two patients younger than 3 years at diagnosis are long-term survivors. Clustering analysis of methylation array data from 18 cases classified tumors as IDH (n = 3, 17 %), G34 (n = 4, 22 %), mesenchymal (n 3, 17= %), and RTK I 'PDGFRA' (n = 8, 44 %). No tumors were classified as K27 subgroup. *PDGFRA* was the most

Correspondence to: Alberto Broniscer, alberto.broniscer@stjude.org.

Electronic supplementary material The online version of this article (doi:10.1007/s00401-015-1532-y) contains supplementary material, which is available to authorized users.

commonly amplified oncogene in 4 of 22 tumors (18 %). *H3F3A* p.G34 occurred in all cases classified as G34. Two of 3 cases in the IDH subgroup had *IDH1* p.R132H. No *H3F3A* p.K27 M, *IDH2* p.R172, or *BRAF* p.V600E mutations were observed. There was a trend towards improved survival in the IDH subgroup ($P = 0.056$). Patients with bithalamic involvement had worse outcomes ($P = 0.019$). Despite some overlap, the molecular features of pediatric GC are distinct from its adult counterpart. Like in adults, the similarity of genetic and epigenetic characteristics with other infiltrative high-grade gliomas suggests that pediatric GC does not represent a distinct molecular entity.

Keywords

Children; DNA methylation profiles; Gliomatosis cerebri; Molecular classification

Introduction

Gliomatosis cerebri (GC), a rare central nervous system (CNS) neoplasm, is defined as a diffuse glioma involving at least three cerebral lobes, frequently bilaterally, and often extending to infra-tentorial structures and even the spinal cord [8]. Although GC affects predominantly adults [8], multiple case reports and a few small series have described its occurrence in children [1, 5, 9, 22].

GC remains one of the deadliest and least understood CNS neoplasms [1, 5, 7, 9, 11, 22, 28]. Although radiological criteria to diagnose GC are well established [8], the evaluation of tumor involvement based on magnetic resonance imaging (MRI) T_2-weighted and/or FLAIR sequences can be subjective. Furthermore, the definition of GC is suitable for neoplasms arising within the cerebral cortex but does not adequately address those originating from deep-seated midline structures. The degree of involvement of gray and/or white matter also varies among affected patients [5]. Finally, it remains uncertain whether GC represents a separate clinical and molecular entity or simply represents the extreme spectrum of infiltrative gliomas [8, 12]. Because of its rarity and the lack of suitable tissue [8], molecular analysis of GC in adults consisted mostly of targeted gene sequencing and copy number abnormalities [7, 11, 12, 17, 19, 21, 25, 28]. A recent study, which utilized DNA methylation analysis to assess molecular subgroups and copy number abnormalities, reported that GC in adults was not a distinct molecular entity because its genetic and epigenetic characteristics resembled those found in other high-grade gliomas [12]. Minimal knowledge is available about the molecular characteristics of pediatric GC [5, 7, 17, 21].

In this study, we report detailed clinical and radiological data and provide for the first time extensive molecular analysis in the largest cohort to date of children with GC.

Materials and methods

Following institutional review board approval, we retrospectively reviewed the clinical and radiological characteristics of all patients younger than 22 years with newly diagnosed primary GC treated at our institution from March 1999 until August 1, 2014. Cases of secondary GC following progression of a pre-existing tumor were excluded.

Detailed clinical and therapy-related data were collected for all patients. Brain MRIs at diagnosis of suspected cases were selected by a neuro-oncologist (AB) and then independently reviewed by a neuro-radiologist (SH). Information was gathered about primary tumor location, presence of mass effect (i.e., type 2 GC), leptomeningeal spread, enhancing areas, and hydrocephalus. The pattern and extent of involvement were assessed by scoring affected cerebral lobes and deep-seated structures (i.e., insula, lentiform nucleus, caudate nucleus, thalamus, brainstem, and cerebellum). A score of 1 was attributed to involvement of each unilateral structure, the brainstem, and cerebellum. Extent of involvement was assessed by T_2-weighted and/or FLAIR MRI sequences. Assessment of the presence of tumor mass was based on T_1- and T_2-weighted/FLAIR signal characteristics independent of the presence of contrast enhancement. All cases underwent histological review by a board-certified neuro-pathologist (BAO) according to the 2007 World Health Organization classification.

Molecular studies

Molecular analysis was performed in tumor samples obtained at diagnosis except for three patients where tissue was only available at progression (n 2) or at autopsy (n = 1). DNA was extracted from formalin-fixed paraffin-embedded (FFPE) tissue using the Maxwell® 16 Plus LEV DNA purification kit (Promega, Madison, WI) according to the manufacturer's instructions. DNA was quantified using the Qubit dsDNA BR assay kit (ThermoFisher Scientific, Grand Island, NY).

Targeted sequencing of *BRAF* p.V600E, *H3F3A* p.K27M, *H3F3A* p.G34, *IDH1* p.R132, and *IDH2* p.R172 was performed. Polymerase chain reaction (PCR) amplification was performed using previously described primers [10, 18, 29, 31]. Direct sequencing of the PCR products was performed using BigDye Terminator v1.1 chemistry on a 3530XL sequencer (Applied Biosystems, Foster City, CA). Tumor and germline samples from five patients included in this study had already undergone whole genome (n = 2), exome (n = 4), and RNA sequencing (n = 3) as part of the Pediatric Cancer Genome Project [30].

Dual-color FISH was performed as previously described to assess copy number abnormalities in *PDGFRA* [4].

Illumina infinium human 450 k bead array

FFPE-derived genomic DNA (500 ng) was treated with bisulfite using the Zymo EZ DNA Methylation Kit (Zymo Research, Irvine, CA) according to the following thermo-cycling conditions (16 cycles; 95 °C for 30 s and 50 °C for 1 h). Following treatment with bisulfite, DNA samples were desulphonated, column purified, then eluted using 12 μL of elution buffer (Zymo Research, Irvine, CA). DNA samples were then processed using the Illumina Infinium HD FFPE Restore kit (Illumina, San Diego, CA) according to the manufacturer's protocol. Following restoration, bisulfite-converted DNA was then processed using the Illumina Infinium Methylation Assay including hybridization to HumanMethylation450 BeadChips (Illumina, San Diego, CA), single base extension assay, staining, and scanning using the Illumina HiScan system according to the manufacturer's recommendations. Beta values representing the fraction of methylated cytosine present at each CpG site were

calculated using the Illumina Genome Studio software (Illumina, San Diego, CA) using the default settings.

Analysis of DNA methylation data was performed using the open source statistical programming language R [23]. Files with raw data generated by the iScan microarray scanner (Illumina, San Diego, CA) were read and processed using the *minfi* Bioconductor package as described in the Illumina GenomeStudio software (Illumina, San Diego, CA) [2]. Further filtering the probes was done as previously described [26]. In total, 438,370 probes were kept for clustering analysis. To determine the subgroup affiliation of our cohort by methylation array, we used previously published data of DNA methylation in pediatric high-grade gliomas as a reference ($n = 59$; GSE36278) [26]. Missing values were imputed using a k-nearest neighbor algorithm [27]. To determine the cluster assignment of a subject from our cohort, the methylation data from each subject was combined with the 59 cases in the reference set for unsupervised consensus clustering as previously described [26]. Briefly, the 8000 most variable methylated CpG probes as measured by standard deviation across combined samples were selected. The consensus matrix was calculated using the k-means algorithm on a fraction of probes (0.8) in 1000 iterations (R package: ConsensusClusterPlus) [20, 26]. Subgroup assignment of each case from our cohort was then resolved from the consensus with the number of subgroups set at 5, corresponding to the number of distinct DNA methylation subgroups identified in a separate cohort of pediatric high-grade gliomas [26].

Analysis of copy number abnormalities based on the 450 k Infinium methylation array was performed using the *conumee* Bioconductor package in default settings [13]. The combined intensities of all available CpG probes were normalized against 12 control samples from normal brain tissue using a linear-regression approach. Detection of amplification and chromosomal gains and losses was performed by manual assessment of the respective loci for each individual profile following automatic scoring [12, 26].

A logistic regression model to estimate the probability of MGMT promoter methylation from the 450 k methylation array was performed as previously described [3].

Other statistical analyses

Descriptive statistical analyses were used to summarize the demographic and clinical characteristics of the patients. Overall survival (OS) was defined as the interval between date of diagnosis and death. Patients who were alive were censored at the time of last contact. To assess for associations with OS, Cox models were used for continuous variables and two-sided log-rank tests were used for categorical variables. The associations between chromosomal gains or losses and methylation subgroups were determined by Fisher's exact tests.

Results

We identified 32 patients [17 (53 %) females] with GC (Table 1). The median age at diagnosis was 10.2 years (range 1.5–19.1). The median latency from onset of symptoms to diagnosis was 60 days (range 7 days–3 years). Twenty-one (66 %) patients presented with

seizures, which were commonly difficult to control. Only two patients had not experienced seizures at their last follow-up. Two patients had a cancer predisposition syndrome consisting of either a monoallelic or biallelic germline mutation (constitutional mismatch-repair deficiency syndrome) of *MSH6* [30] (Table 1).

Twenty-three (72 %) patients had type 1 and 9 (28 %) type 2 primary GC (Table 1). A median of 4 (range 3–8) cerebral lobes and 9.5 (range 3–15) brain structures was affected at diagnosis (Table 1). Twenty-five (78 %) patients had at least one thalamus affected. In addition, 9 (28 %) patients displayed symmetrical involvement of both thalami typical of bithalamic gliomas; all had biopsies obtained from one of the thalami to corroborate the impression that this was a prominent component of the tumor. Ten (31 %) patients had predominant involvement of gray matter, 9 (28 %) of white matter, and 13 (41 %) showed equal involvement of both. Twelve of 31 patients (39 %) had hydrocephalus at diagnosis; one patient was not evaluable for new onset hydrocephalus due to a VP shunt previously inserted for an unrelated disorder. Only 1 of 32 evaluable patients displayed metastatic disease at diagnosis. Fifteen tumors contained areas of focal enhancement, 7 of them corresponding to cases of type 2 GC. All cases of type 2 GC had unambiguous focal areas with distinct signal characteristics from the surrounding tumor with ($n = 7$) or without ($n = 2$) contrast enhancement.

All tumors represented astrocytic neoplasms with diffuse infiltration of the surrounding brain parenchyma. Of 30 pure astrocytomas, 4 were grade II, 22 grade III, and 4 grade IV (Table 1). Two tumors were not easy to classify histologically due to the concomitant presence of both an astrocytic and a minor neuronal component (patients 28 and 31 in Table 1). Patient 28 (Table 1) with a low-grade glioneuronal tumor developed leptomeningeal spread at progression and malignant transformation into a glioblastoma was confirmed at autopsy.

Molecular studies

Unsupervised consensus clustering analysis of genome-wide DNA methylation was conducted in 18 (56 %) patients with adequate tissue. By comparing to a previously published dataset of pediatric high-grade gliomas, our cohort was classified into four subgroups: IDH ($n = 3$, 17 %), G34 ($n = 4$, 22 %), mesenchymal ($n = 3$, 17= %), and RTK I ‘PDGFRA’ ($n = 8$, 44 %) (Fig. 1; Table 2). A subgroup representing H3.3 K27M-mutated tumors was not observed. Seven of 18 (39 %) tumors displayed MGMT promoter methylation. MGMT promoter methylation occurred in all methylation subgroups except for mesenchymal (Table 2).

Sequencing of hotspot mutations was available for a maximum of 25 (78 %) tumors. Whereas 5 of 21 (24 %) tumors displayed *H3F3A* p.G34, no *H3F3A* p.K27 M mutations were observed. All four *H3F3A* p.*G34R*-mutated tumors with methylation data clustered in the G34 subgroup. Only 2 of 25 (8 %) tumors, both type 2 GC involving the frontal lobes, harbored *IDH1* p.R132H mutations. Only one case assigned to the IDH subgroup by methylation did not harbor this mutation by targeted sequencing. Although no *BRAF* p.V600E mutations were detected, one patient harbored multiple abnormalities (*BRAF* T589I, G596D; R603*) previously described in this gene (http://cancer.sanger.ac.uk/cosmic)

(Table 2). Among five subjects who had previously undergone genome-wide sequencing, *PDGFRA* and *TP53* mutations were demonstrated in 1 and 2 tumors, respectively [30]. A fusion between *TPM3* and *NTRK1* was demonstrated in one case [30] (Table 2).

Multiple amplified oncogenes were observed, the most common of which was *PDGFRA* seen in 4 of 22 cases (18 %) (Table 2). Other amplified oncogenes included *MDM4* ($n = 2$), *CDK4* ($n = 1$), *MYC* ($n = 1$), and *MYCN* ($n = 1$). *CDKN2A* deletion was observed in 2 of 22 cases (9 %). The most common areas of large gains in 18 tumors were 1q (33 %), 2p (33 %), 2q (39 %), chromosome 7 (44 %), and 12p (22 %). Likewise, the most common areas of large chromosomal losses were 3q (28 %), 6q (22 %), 9p (22 %), 10q (28 %), and 13q (28 %). Concomitant loss of 1p and 19q was not observed.

Multiple associations were found between large areas of chromosomal gains or losses and methylation subgroups (Supplemental Fig. 1). Whereas large gains of 2p and 2q were associated with the RTK I 'PDGFRA' subgroup ($P = 0.012$ and $P = 0.042$, respectively), losses of 4q and 9p were associated with the G34 subgroup ($P = 0.045$ and $P = 0.021$, respectively). Gains of chromosome 7 were observed exclusively in the RTK I 'PDGFRA' subgroup except for 2 cases ($P = 0.02$).

Outcome

Despite aggressive therapy, only two patients with GC diagnosed before 3 years of age are long-term survivors; both experienced tumor progression after chemotherapy and required radiation therapy (Table 1). The median OS for all patients was 16.5 months (range 4.7–87.7+ months). None of the continuous variables analyzed, including age at diagnosis, interval from onset of symptoms and diagnosis, number of cerebral lobes or brain structures affected were associated with OS. Likewise, gender, presence of seizures at presentation, type 1 vs. type 2 GC, presence of contrast enhancement, histological grade, and MGMT promoter status were not associated with OS (Supplemental Figs. 2–5). Patients with symmetrical bithalamic involvement had a worse survival ($P = 0.0196$) (Fig. 2a). Although it did not reach statistical significance, there was a borderline association between methylation subgroups and outcome (Fig. 2b). Specifically, patients in the IDH subgroup seemed to fare better than those in the other subgroups ($P = 0.056$).

Discussion

Despite the use of aggressive therapy, GC still portends one of the poorest prognoses of all pediatric CNS cancers, probably only surpassed by diffuse intrinsic pontine gliomas [14]. We report clinicopathologic and radiological characteristics in the largest cohort to date of pediatric GC. More importantly, we provided for the first time detailed molecular information about this cancer. We showed that GC in children harbors mutations, oncogene amplifications, and particularly a methylation profile that corresponds to other pediatric high-grade gliomas [16, 24, 26, 30]. *H3F3A* p.G34 mutations, which were perfectly captured by methylation analysis, were seen mostly in adolescents with predominant involvement of cortical lobes and accounted for 15 % of cases. *IDH1* p.R132 or clustering in the IDH methylation subgroup was seen in less than 10 % of tumors, all arising in the frontal lobe of patients at least 10 years old. The lack of *BRAF* p.V600E in our patients' tumors is

important and suggests that children with GC will not be good candidates for therapy with BRAF inhibitors. The K27 methylation subgroup, which accounts for the largest group of pediatric high-grade gliomas [16, 26], was conspicuously absent from our cohort. This finding may seem intuitive since the definition of GC is based on tumor involvement of cerebral lobes and *H3F3A* p.K27 M predominantly affects midline tumors [24, 26, 29]. However, we showed that children with GC commonly have involvement of deeper brain structures, including the thalami. Furthermore, similar to other studies in children [1, 5, 6], we showed that more than 25 % of our patients had symmetrical bithalamic involvement as a prominent feature of GC. Because only 4 of our 9 patients with GC and a symmetrical bithalamic involvement had molecular data available, the possibility that a *H3F3A* p.K27M mutation could be found in pediatric GC cannot be entirely excluded.

Our analysis of copy number abnormalities showed amplifications of several oncogenes previously found in other pediatric high-grade gliomas, including *PDG-FRA*, *CDK4*, and *MDM4* [24, 26, 30]. Similarly, *MYC* and *MYCN* amplifications observed in one case each had been occasionally observed in pediatric high-grade gliomas [30].

Not surprisingly, we identified molecular differences between GC in children and their adult counterparts. Whereas the IDH subgroup was uncommon in children, it accounted for approximately half the cases of adult GC [12, 17, 25]. In contrast to our results, approximately half of adult cases in the IDH subgroup represented oligodendrogliomas with concomitant 1p and 19q loss [12]. Unlike adult cases of GC and similar to a previous study of high-grade gliomas across all age groups [12, 26], the RTK II subgroup was not observed in our patients. Interestingly, we reported associations between specific areas of chromosomal gains or losses and the RTK I ‘PDGFRA’ and G34 methylation subgroups. Since some of these chromosomal areas (e.g., 9p, 7q) harbor oncogenes or tumor suppressor genes that are key in glioma tumorigenesis, these associations should be further studied.

We confirmed multiple clinical findings previously described in children with GC, including the common occurrence of seizures, which were frequently difficult to control and often presented as status epilepticus [1, 5, 15]. The long interval from onset of symptoms and histological confirmation in a subset of patients with GC had also been previously reported and can be attributed to the challenges in establishing this diagnosis [15]. One of the main limitations of our study was the lack of suitable tissue for more detailed molecular analysis in all patients’ samples.

The OS of our patients was shorter than that reported in some adult studies but comparable to the previously reported pediatric experience [5, 7, 12, 21, 28]. Similar to previous studies [12, 16, 17, 21, 26], there was a suggestion that children with GC in the IDH methylation subgroup might fare better than those in the other groups since our three patients survived for at least 1.5 years without disease progression. However, no generalizable conclusions can be drawn based on such small number of patients. We hypothesize that the association between bithalamic involvement and worse outcome may be due to larger tumor burden but a potential role of tumor biology cannot be excluded. Unlike a previous adult study [12], MGMT promoter methylation status was not prognostic in our patients. This was likely due to the fact that only one-third of our patients received upfront therapy containing

temozolomide. Interestingly, our only two long-term survivors were younger than 3 years at diagnosis including one patient with a *TPM3* and *NTRK1* fusion [30].

A recent report raised the possibility that GC in adults may not represent a separate brain tumor entity based on overlapping genetic and epigenetic characteristics with other gliomas [12]. Likewise, the overlap of molecular characteristics between GC and other high-grade gliomas in children suggests that the same may apply to pediatric GC.

Supplementary Material

Refer to Web version on PubMed Central for supplementary material.

Acknowledgments

This work was supported by the United States National Institutes of Health Cancer Center Support (CORE) Grant P30 CA21765 and by the American Lebanese Syrian Associated Charities (ALSAC). We thank Geoffrey Neale and John Morris for assistance in performing the methylation studies. We thank Racquel Collins for her assistance in performing targeted sequencing.

References

1. Armstrong GT, Phillips PC, Rorke-Adams LB, Judkins AR, Localio AR, Fisher MJ. Gliomatosis cerebri: 20 years of experience at the Children's Hospital of Philadelphia. Cancer. 2006; 107:1597–1606. DOI: 10.1002/cncr.22210 [PubMed: 16955507]
2. Aryee MJ, Jaffe AE, Corrada-Bravo H, Ladd-Acosta C, Feinberg AP, Hansen KD, Irizarry RA. Minfi: a flexible and comprehensive Bioconductor package for the analysis of Infinium DNA methylation microarrays. Bioinformatics. 2014; 30:1363–1369. DOI: 10.1093/bioinformatics/btu049 [PubMed: 24478339]
3. Bady P, Sciuscio D, Diserens AC, et al. MGMT methylation analysis of glioblastoma on the Infinium methylation Bead-Chip identifies two distinct CpG regions associated with gene silencing and outcome, yielding a prediction model for comparisons across datasets, tumor grades, and CIMP-status. Acta Neuropathol. 2012; 124:547–560. DOI: 10.1007/s00401-012-1016-2 [PubMed: 22810491]
4. Broniscer A, Tatevossian RG, Sabin ND, Klimo P Jr, Dalton J, Lee R, Gajjar A, Ellison DW. Clinical, radiological, histological and molecular characteristics of paediatric epithelioid glioblastoma. Neuropathol Appl Neurobiol. 2014; 40:327–336. DOI: 10.1111/nan.12093 [PubMed: 24127995]
5. Chappé C, Riffaud L, Tréguier C, et al. Primary gliomatosis cerebri involving gray matter in pediatrics: a distinct entity? A multicenter study of 14 cases. Childs Nerv Syst. 2013; 29:565–571. DOI: 10.1007/s00381-012-2016-1 [PubMed: 23306961]
6. Colosimo C, di Lella GM, Tartaglione T, Riccardi R. Neuroimaging of thalamic tumors in children. Childs Nerv Syst. 2002; 18:426–439. DOI: 10.1007/s00381-002-0607-y [PubMed: 12192502]
7. D'Urso OF, D'Urso PI, Marsigliante S, Storelli C, Luzi G, Gianfreda CD, Montinaro A, Distante A, Ciappetta P. Correlative analysis of gene expression profile and prognosis in patients with gliomatosis cerebri. Cancer. 2009; 115:3749–3757. DOI: 10.1002/cncr.24435 [PubMed: 19517475]
8. Fuller, GN.; Kros, JM. Gliomatosis cerebri. In: Louis, DN.; Ohgaki, H.; Wiestler, OD.; Cavenee, WK., editors. WHO classification of tumours of the central nervous system. 4th. IARC; Lyon: 2007. p. 50-52.
9. George E, Settler A, Connors S, Greenfield JP. Pediatric gliomatosis cerebri: a review of 15 Years. J Child Neurol. 2015; doi: 10.1177/0883073815596612
10. Hartmann C, Meyer J, Balss J, et al. Type and frequency of IDH1 and IDH2 mutations are related to astrocytic and oligodendroglial differentiation and age: a study of 1,010 diffuse gliomas. Acta Neuropathol. 2009; 118:469–474. DOI: 10.1007/s00401-009-0561-9 [PubMed: 19554337]

11. Herrlinger U, Felsberg J, Küker W, et al. Gliomatosis cerebri: molecular pathology and clinical course. Ann Neurol. 2002; 52:390–399. DOI: 10.1002/ana.10297 [PubMed: 12325066]
12. Herrlinger U, Jones DT, Glas M, et al. Gliomatosis cerebri: no evidence for a separate brain tumor entity. Acta Neuropathol. 2015; in press. doi: 10.1007/s00401-015-1495-z
13. Hovestadt, V.; Zapatka, M. *conumee*: enhanced copy-number variation analysis using Illumina 450 k methylation arrays. Bioconductor: open source software for bioinformatics. R package version 0.99.4http://www.bioconductor.org/packages/release/bioc/html/conumee.html. Accessed 1 Sept 2015
14. Jackson S, Patay Z, Howarth R, Pai Panandiker AS, Onar-Thomas A, Gajjar A, Broniscer A. Clinico-radiologic characteristics of long-term survivors of diffuse intrinsic pontine glioma. J Neurooncol. 2013; 114:339–344. DOI: 10.1007/s11060-013-1189-0 [PubMed: 23813229]
15. Jennings MT, Frenchman M, Shehab T, Johnson MD, Creasy J, LaPorte K, Dettbarn WD. Gliomatosis cerebri presenting as intractable epilepsy during early childhood. J Child Neurol. 1995; 10:37–45. DOI: 10.1177/088307389501000111 [PubMed: 7539465]
16. Korshunov A, Ryzhova M, Hovestadt V, et al. Integrated analysis of pediatric glioblastoma reveals a subset of biologically favorable tumors with associated molecular prognostic markers. Acta Neuropathol. 2015; 129:669–678. DOI: 10.1007/s00401-015-1405-4 [PubMed: 25752754]
17. Kwon MJ, Kim ST, Kwon MJ, et al. Mutated IDH1 is a favorable prognostic factor for type 2 gliomatosis cerebri. Brain Pathol. 2012; 22:307–317. DOI: 10.1111/j.1750-3639.2011.00532 [PubMed: 21929658]
18. Lee X, Gao M, Ji Y, Yu Y, Feng Y, Li Y, Zhang Y, Cheng W, Zhao W. Analysis of differential BRAF(V600E) mutational status in high aggressive papillary thyroid microcarcinoma. Ann Surg Oncol. 2009; 16:240–245. DOI: 10.1245/s10434-008-0233-3 [PubMed: 19034577]
19. Min HS, Kim B, Park SH. Array-based comparative genomic hybridization and immunohistochemical studies in gliomatosis cerebri. J Neurooncol. 2008; 90:259–266. DOI: 10.1007/s11060-008-9665-7 [PubMed: 18704270]
20. Monty S, Tamayo P, Mesirov J, Golub T. Consensus clustering: a resampling-based method for class discovery and visualization of gene expression microarray data. Mach Learn. 2003; 52:91–118.
21. Narasimhaiah D, Miquel C, Verhamme E, Desclée P, Cosnard G, Godfraind C. IDH1 mutation, a genetic alteration associated with adult gliomatosis cerebri. Neuropathology. 2012; 32:30–37. DOI: 10.1111/j.1440-1789.2011.01216.x [PubMed: 21481010]
22. Perkins GH, Schomer DF, Fuller GN, Allen PK, Maor MH. Gliomatosis cerebri: improved outcome with radiotherapy. Int J Radiat Oncol Biol Phys. 2003; 56:1137–1146. DOI: 10.1016/S0360-3016(03)00293-1 [PubMed: 12829152]
23. R Core Team. R: a language and environment for statistical computing. R Foundation for Statistical Computing; Vienna, Austria: 2015. https://www.R-project.org/. Accessed 1 Sept 2015
24. Schwartzentruber J, Korshunov A, Liu XY, et al. Driver mutations in histone H3.3 and chromatin remodelling genes in paediatric glioblastoma. Nature. 2012; 482:226–231. DOI: 10.1038/nature10833 [PubMed: 22286061]
25. Seiz M, Tuettenberg J, Meyer J, Essig M, Schmieder K, Mawrin C, von Deimling A, Hartmann C. Detection of IDH1 mutations in gliomatosis cerebri, but only in patients with additional solid component: evidence for molecular subtypes. Acta Neuropathol. 2010; 120:261–267. DOI: 10.1007/s00401-010-0701-2 [PubMed: 20514489]
26. Sturm D, Witt H, Hovestadt V, et al. Hotspot mutations in H3F3A and IDH1 define distinct epigenetic and biological subgroups of glioblastoma. Cancer Cell. 2012; 22:425–437. DOI: 10.1016/j.ccr.2012.08.024 [PubMed: 23079654]
27. Troyanskaya O, Cantor M, Sherlock G, Brown P, Hastie T, Tibshirani R, Botstein D, Altman RB. Missing value estimation methods for DNA microarrays. Bioinformatics. 2001; 17:520–525. DOI: 10.1093/bioinformatics/17.6.520 [PubMed: 11395428]
28. Ware ML, Hirose Y, Scheithauer BW, Yeh RF, Mayo MC, Smith JS, Chang S, Cha S, Tihan T, Feuerstein BG. Genetic aberrations in gliomatosis cerebri. Neurosurgery. 2007; 60:150–158. DOI: 10.1227/01.NEU.0000249203.73849.5D [PubMed: 17228264]

29. Wu G, Broniscer A, McEachron TA, St. Jude Children's Research Hospital-Washington University Pediatric Cancer Genome Project. et al. Somatic histone H3 alterations in pediatric diffuse intrinsic pontine gliomas and non-brainstem glioblastomas. Nat Genet. 2012; 44:251–253. DOI: 10.1038/ng.1102 [PubMed: 22286216]

30. Wu G, Diaz AK, Paugh BS, St. Jude Children's Research Hospital-Washington University Pediatric Cancer Genome Project. et al. The genomic landscape of diffuse intrinsic pontine glioma and pediatric non-brainstem high-grade glioma. Nat Genet. 2014; 46:444–450. DOI: 10.1038/ng.2938 [PubMed: 24705251]

31. Zhang J, Wu G, Miller CP, St. Jude Children's Research Hospital-Washington University Pediatric Cancer Genome Project. et al. Whole-genome sequencing identifies genetic alterations in pediatric low-grade gliomas. Nat Genet. 2013; 45:602–612. DOI: 10.1038/ng.2611 [PubMed: 23583981]

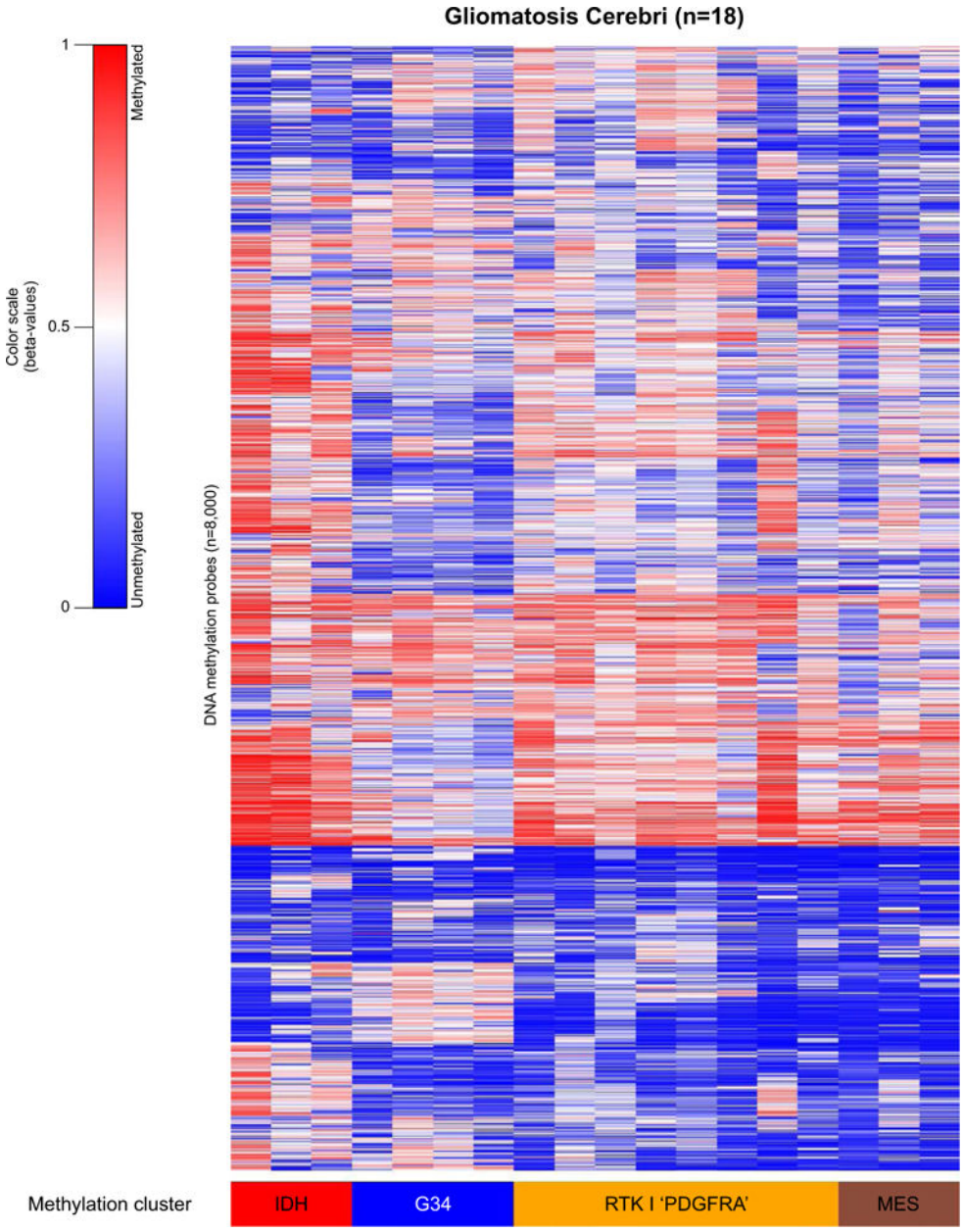

Fig. 1.

Heatmap representation of unsupervised consensus clustering analysis of 450 k methylation array profiles in 18 pediatric patients with gliomatosis cerebri using the 8000 most variable methylated CpG probes. *MES* mesenchymal

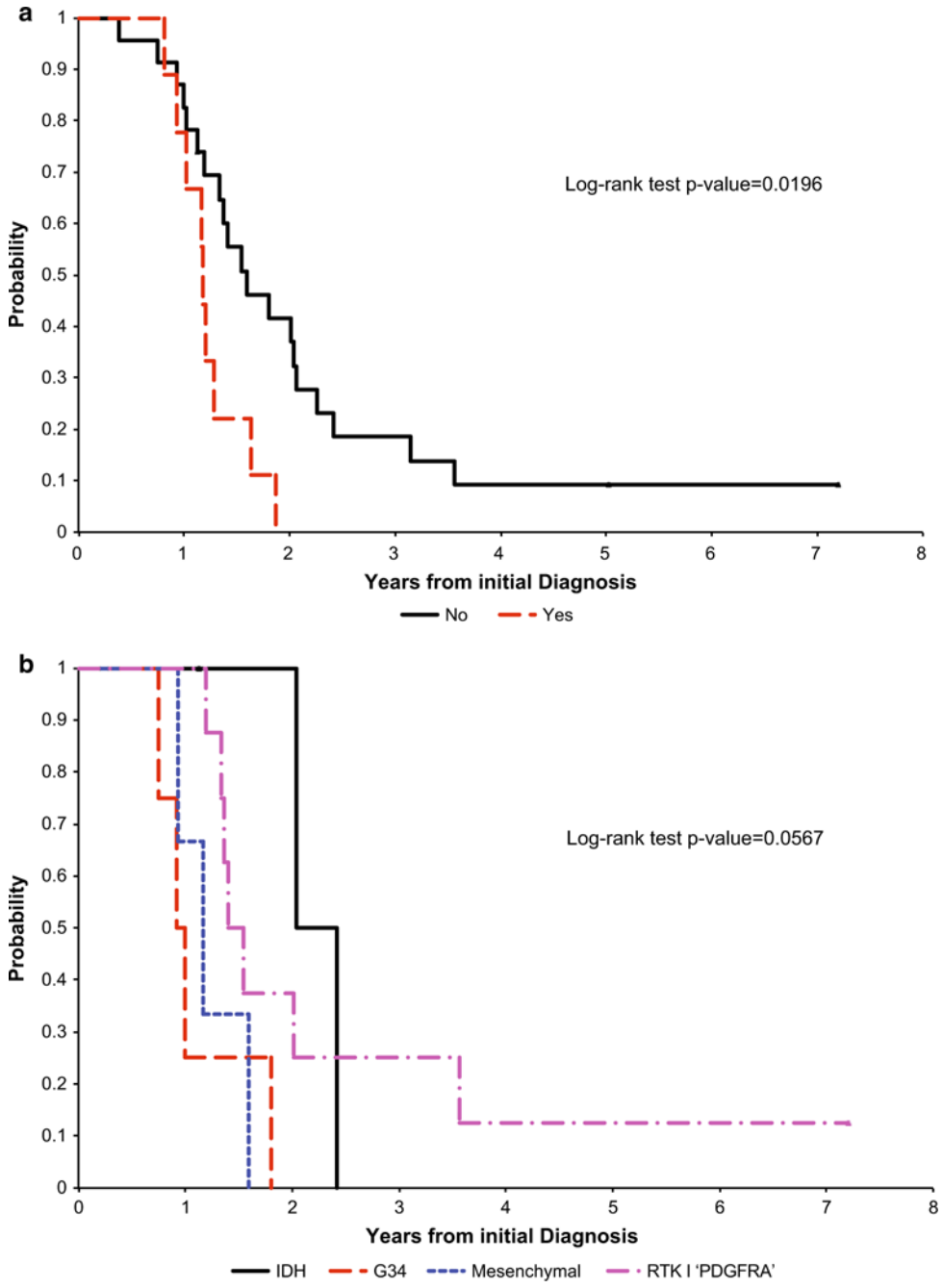

Fig. 2.

a Overall survival of 32 pediatric patients with gliomatosis cerebri based on the presence of symmetrical bithalamic involvement. **b** Overall survival of 18 pediatric patients with gliomatosis cerebri based on the methylation subgroups

Table 1

Clinical, radiological, and histological characteristics of all patients

Patient	Age at diagnosis (years)/ gender	Race/ethnicity	Type of GC/no. of cerebral lobes involved[d]	Bithalamic involvement	Histological diagnosis/surgery	Therapy	Survival (yrs)
1	5.6/F	Caucasian	Type 1/4	Yes	AA/biopsy	RT	0.8
2	4.3/M	Caucasian	Type 1/7	Yes	AA/biopsy	RT + chemo	1.3
3	13.7/M	Mixed race	Type 1/6	No	AA/PR	RT + chemo	1.4
4	14.5/M	Caucasian	Type 1/5	No	AA/biopsy	RT + chemo	3.1
5	16.3/M	Caucasian	Type1/4	Yes	DA (grade II)/biopsy	RT + chemo	1.2
6	6.6/M	Caucasian	Type 1/4	Yes	DA (grade II)/biopsy	RT + chemo	1.6
7	9.1/M	Caucasian	Type 1/6	No	AA/PR	RT + chemo	2.6
8	5.5/F	Caucasian	Type 1/3	No	DA (grade II)/biopsy	RT + chemo	1.5
9	16.5/F	Caucasian	Type 1/4	No	AA/biopsy	RT + chemo	1.2
10	10/M	Caucasian	Type 2/5	No	GBM/PR	RT + chemo	2.4
11[b]	9.9/F	African-American	Type 2/8	No	GBM/PR	RT + chemo	1.1
12	10.4/F	Hispanic	Type 1/6	No	AA/biopsy	RT + chemo	2.1
13	6.3/F	Caucasian	Type 2/4	Yes	AA/biopsy	RT + chemo	1
14	1.5/F	Caucasian	Type 2/3	No	DA (grade II)/biopsy	Chemo	1.6
15	19.1/M	Caucasian	Type 2/3	No	AA/STR	RT + chemo	2
16	12.3/F	Caucasian	Type 1/5	No	AA/biopsy	RT + chemo	0.9
17	4.8/M	Caucasian	Type 1/4	No	AA/biopsy	RT + chemo	2
18[c]	12.9/F	African-American	Type 1/8	No	AA/PR	RT + chemo	0.4
19	18.8/F	Caucasian	Type 1/8	Yes	AA/biopsy	RT chemo +	1.2
20[a]	6.5/M	African-American	Type 2/3	Yes	AA/biopsy	RT + chemo	0.9
21	16.6/F	Mixed race	Type 1/4	No	GBM/PR	RT + chemo	1
22	8.4/F	Hispanic	Type 1/3	Yes	AA/biopsy	RT + chemo	1.2
23	15/F	African-American	Type 1/4	Yes	AA/biopsy	RT + chemo	1.9
24	15.7/F	Caucasian	Type 2/4	No	GBM/STR	RT + chemo	1.3
25	16.8/M	Caucasian	Type 1/4	No	AA/biopsy	RT + chemo	1.8
26	12.4/M	Hispanic	Type 1/6	No	AA/biopsy	RT + chemo	1.4
27	8.4/M	African-American	Type 1/3	No	AA/biopsy	RT + chemo	0.7

Patient	Age at diagnosis (years)/ gender	Race/ethnicity	Type of GC/no. of cerebral lobes involved[d]	Bithalamic involvement	Histological diagnosis/surgery	Therapy	Survival (yrs)
28	10/F	Mixed race	Type 1/5	No	Low-grade glioneuronal tumor/PR	RT + chemo	3.6
29	12/M	Caucasian	Type 1/3	No	AA/biopsy	RT + chemo	1
30	1.8/F	Caucasian	Type 1/5	No	AA/STR	RT + chemo	5+
31	2.7/M	Caucasian	Type 2/4	No	Malignant glioneuronal tumor/STR	RT + chemo	7.2+
32[b]	12.9/F	Caucasian	Type 2/7	No	AA/biopsy	RT	1.4+

No. number, *F* female, *M* male, *AA* anaplastic astrocytoma, *GBM* glioblastoma, *DA* diffuse astrocytoma, *PR* partial resection, *STR* subtotal resection, *RT* radiation therapy, *chemo* chemotherapy

[a] Only patient 20 had leptomeningeal spread at diagnosis requiring craniospinal RT

[b] Patients 11 and 32 had monoallelic or biallelic germline mutations of *MSH6*, respectively

[c] All deaths were due to progressive disease except for patient 18 who died of treatment complications

[d] Unilateral involvement of frontal, temporal, parietal, and occipital lobes each constituted a unit in this measurement. Maximum score = 8

Table 2

Molecular characteristics of evaluable tumors

Patient	Methylation subgroup	MGMT promoter methylation	*IDH1* p.R132H	*H3F3A* p.G34	*CDKN2A* Loss	*PDGFRA* ampl	Other relevant molecular abnormalities
3	RTK I 'PDGFRA'	Unmethylated	No	No	No	No	No
4	NA	NA	No	No	NA	No	NA
8	RTK I 'PDGFRA'	Methylated	No	No	No	No	*CDK4* ampl
9	RTK I 'PDGFRA'	Methylated	No	No	No	No	*MDM4* ampl
10	IDH	Methylated	Yes	No	No	Yes	No
11[a]	NA	NA	No	No	No	No	*PIK3CA* R88Q, *TP53* R248 W, *NF1* L952 fs
13	NA	NA	No	No	NA	NA	*BRAF* T589I, G596D; R603*
14[b]	Mesenchymal	Unmethylated	No	No	No	No	No
15	IDH	Unmethylated	Yes	No	No	No	No
16	G34	Unmethylated	No	Yes	No	No	No
17	RTK I 'PDGFRA'	Unmethylated	No	No	No	Yes	*MDM4*
18[a]	NA	NA	No	No	Yes	No	*PDGFRA* N468S, *BCOR* R1164*
20	Mesenchymal	Unmethylated	No	No	No	Yes	No
21[a]	NA	NA	No	Yes	No	Yes	*TP53* R342*
22	Mesenchymal	Unmethylated	No	No	No	No	No
23	NA	NA	No	No	NA	NA	NA
24[b]	RTK I 'PDGFRA'	Methylated	No	No	No	No	No
25	G34	Unmethylated	No	Yes	No	No	No
26	RTK I 'PDGFRA'	Unmethylated	No	No	No	No	No
27	G34	Methylated	No	Yes	No	No	No
28[b]	RTK I 'PDGFRA'	Unmethylated	No	No	No	No	*MYCN* ampl
29	G34	Methylated	No	Yes	Yes	No	*MYC*
30[a]	NA	NA	No	No	No	No	No
31[a]	RTK I 'PDGFRA'	Unmethylated	No	No	No	No	Fusion between *TPM3* and *NTRK1*
32	IDH	Methylated	No	No	No	No	No

[a] Patients whose tumors previously underwent whole genome/exome/RNA sequencing

[b] Tumor samples available at the time of progression (patients 14 and 24) or at autopsy (patient 28)